Supplementary Material

Regulating d-band electrons of sulfur-enriched CoS_x to weakening the S-Hads bond in CoS_x/ZnCdS Ohmic heterojunctions for enhanced photocatalytic hydrogen evolution

Jiaqi Yang [a, b, c], Yuanjin He [a, b, c], Yuqiang Hao [a, b, c], Xuqiang Hao [a, b, c, *], and Zhiliang Jin[a, b, c]

[a] *School of Chemistry and Chemical Engineering, North Minzu University, Yinchuan 750021, P.R.China*

[b] *Ningxia Key Laboratory of Solar Chemical Conversion Technology, North Minzu University, Yinchuan 750021, P.R.China*

[c] *Key Laboratory for Chemical Engineering and Technology, State Ethnic Affairs Commission, North Minzu University, Yinchuan 750021, P.R.China*

Corresponding author *E-mail address*: haoxuqiang@126.com (X. Q. Hao)

1. Characterizations

The crystal structure was analyzed by X-ray diffraction (XRD) using a Rigaku Ultima III X-ray diffractometer set at 40 kV and 30 mA. The morphology and microstructure of the catalysts were examined through field emission scanning electron microscopy (SEM: JSM-6701F, JEOL, 50 kV), and low-resolution and high-resolution transmission electron microscopy (TEM and HRTEM) images were captured using a JEM-2100 electron microscope operating at 200 kV. X-ray photoelectron spectroscopy (XPS: ESCALAB Xi^+) was employed to determine the elemental composition and valence states of the samples. The zeta potential of the catalyst was measured in pure water using a Litesizer 500. The UV-vis diffuse reflectance spectra (DRS), calibrated with $BaSO_4$ powder, and the UV-vis absorption spectra of all catalysts were recorded using a PerkinElmer Lambda-750 UV-vis-NIR spectrometer. The fluorescence (PL) spectra and time-resolved fluorescence emission spectra of the samples were obtained using a FLUORO-MAX-4 spectrophotometer and a Horiba Jobin Yvon Data Station HUB, respectively.

2. Photocatalytic hydrogen evolution

The photocatalytic hydrogen evolution reaction is carried out using a 64 mL quartz glass bottle in a nine-channel photocatalytic reaction system (Perfect Light-PCX50B Discover). A 5W LED lamp is used as the light source. A dispersion of 6 mg of catalyst in 30 mL of a 10 vol% lactic acid aqueous solution is prepared. Exhaust the air from the glass bottle with N_2. For each measurement, 0.5 mL of gas is extracted and the hydrogen production is analyzed using a GC7900 gas chromatograph (TCD, 13X column).

3. Electrochemical measurement

To perform photoelectrochemical measurements on an electrochemical workstation (Versatat4-400, Advanced Measurement Technology) using a three-electrode cell with a working electrode, Pt serves as the counter electrode and a saturated calomel electrode (SCE) as the reference electrode. Using 0.2M Na_2SO_4 solution as electrolyte. Using a 300W Xe lamp with a 420nm optical cutoff filter as the light source, transient photocurrent measurements were recorded under visible light illumination under open circuit potential. Measure linear sweep voltammetry (LSV) at a scanning rate of 5mV s^{-1} at room temperature. Electrochemical impedance spectroscopy (EIS) is collected at an open circuit potential with a modulation amplitude of 5mV in the frequency range of 1.0MHz to 0.1Hz. Mott Schottky measurements were conducted in the dark, with a bias voltage range of -1.0 V to 1.0 V (relative to SCE) and a frequency of 1000 Hz， and cyclic voltammetry (CV) was determined at a scan rate of 50， 70， 100， 150， 200 mV s^{-1}.

4. DFT calculation

Using first principles, density functional theory (DFT) calculations were performed in the generalized gradient approximation (GGA) using the Perdew Burke Ernzerhof (PBE) formula. In reciprocal space, a 2x5x1 Monkhorst-Pack grid was used along with a smearing parameter of 0.1 eV to calculate electronic structure. The convergence criteria for self-consistent field (SCF) force, and displacement were1.0x10-6 Ha, 3.0 x 10-2 eV/Å, and 1.0 x 10-3 Å respectively. Atomic relaxation was allowed to obtain more accurate results. Ultrasoft pseudopotentials were utilized in this study with a cut-off energy of 500.00 eV.

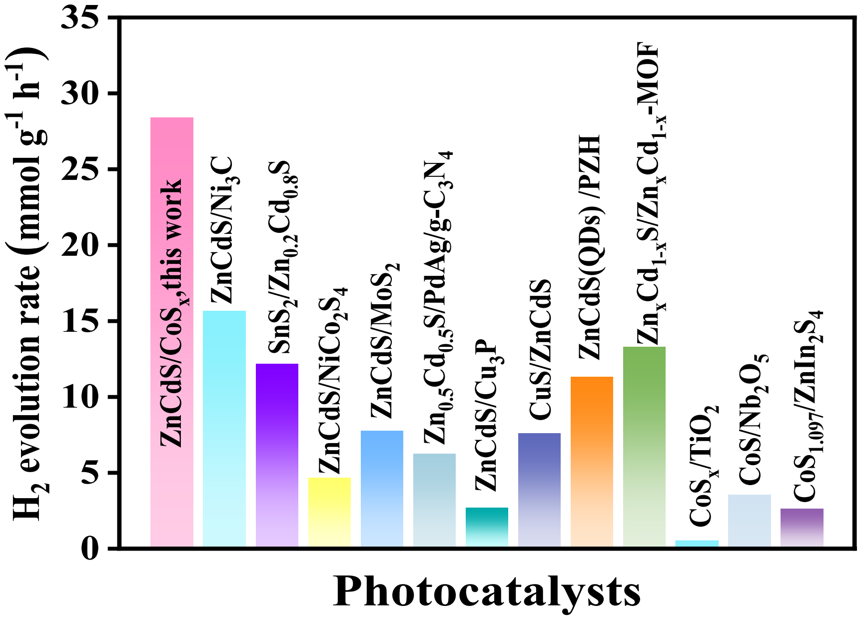

Figure S1. Comparison of photocatalytic hydrogen evolution activity based on ZnCdS and CoS materials.

Table S1 Comparison of photocatalytic hydrogen production experiments based on ZnCdS and CoS materials.

Photocatalysts	**Sacrificial reagent**	**Lamp source**	**Hydrogen production (mmol g^{-1} h^{-1})**	**References**
ZnCdS/CoS_x	10% vol lactic acid	Visible light irradiation	28.40	**This work**
ZnCdS/Ni_3C	0.25M Na_2S/0.25M Na_2SO_3	300 W Xenon lamp	15.66	[1]
SnS_2/$Zn_{0.2}Cd_{0.8}S$	10vol% TEOA	300 W Xenon lamp	12.17	[2]
ZnCdS/$NiCo_2S_4$	0.25M Na_2S/0.35M Na_2SO_3	300 W Xenon lamp	4.67	[3]
ZnCdS/MoS_2	0.25M Na_2S/0.35M Na_2SO_3	CEL-SPH2N automatic online catalytic system	7.76	[4]
$Zn_{0.5}Cd_{0.5}S$/PdAg/g-C_3N_4	10vol% TEOA	300 W Xenon lamp	6.25	[5]
ZnCdS/Cu_3P	0.35M Na_2S/0.25M Na_2SO_3	300 W Xenon lamp	2.70	[6]
CuS/ZnCdS	0.35M Na_2S/0.25M Na_2SO_3	300 W Xenon lamp	7.58	[7]
ZnCdS （QDs）/PZH	10% vol lactic acid	300 W Xenon lamp	11.32	[8]
$Zn_xCd_{1-x}S$/Zn_xCd_{1-x}-MOF	lactic acid and phosphate buffer	300 W Xenon lamp	13.30	[9]
CoS_x/TiO_2	15% vol methanol	300 W Xenon lamp	0.51	[10]
CoS/Nb_2O_5	10vol% TEOA	300 W Xenon lamp	3.55	[11]
$CoS_{1.097}$/$ZnIn_2S_4$	10vol% TEOA	300 W Xenon lamp	2.63	[12]

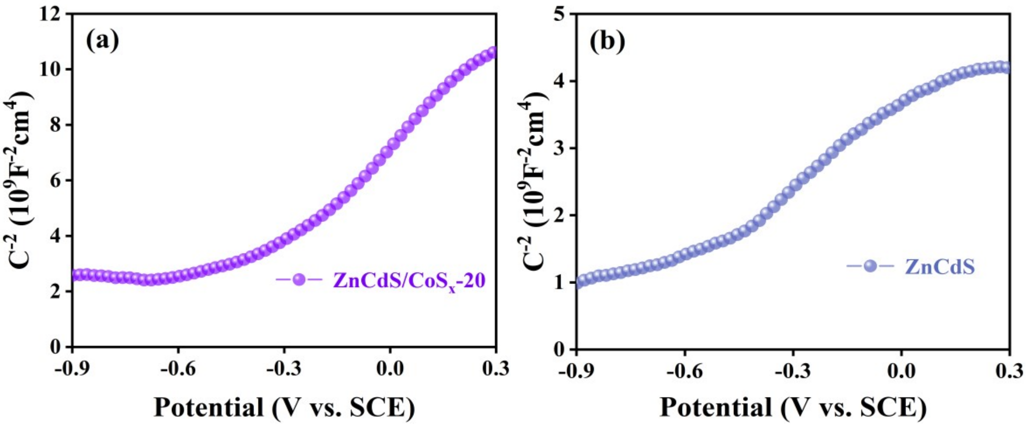

Figure S2. Mott Schottky curve under illumination conditions of (a) ZnCdS/CoS_x-20, (b) ZnCdS.

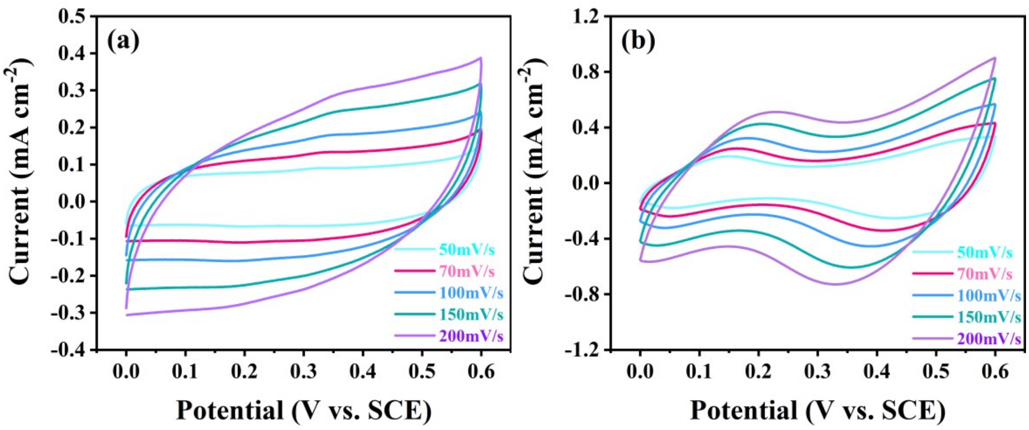

Figure S3. (a) CV curves of (a) ZnCdS and (b) CoS_x at various scan voltage.

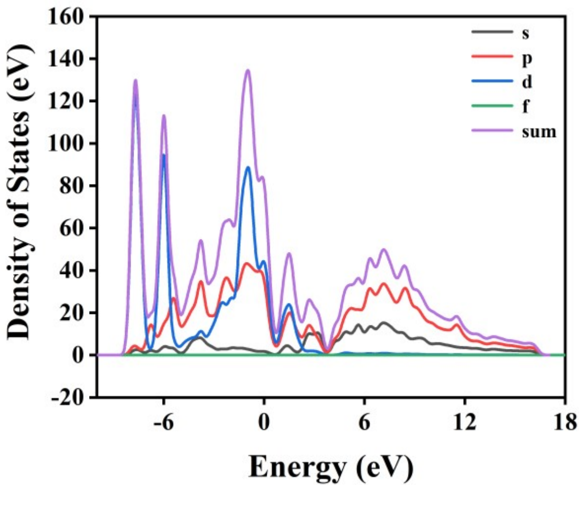

Figure S4. The PDOS of ZnCdS/CoS_x heterojunction.

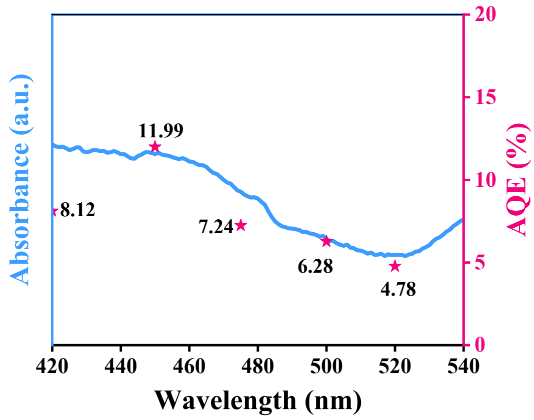

Figure S5. AQE at 420, 450, 475, 500 and 520nm for ZnCdS/CoS_x-20.

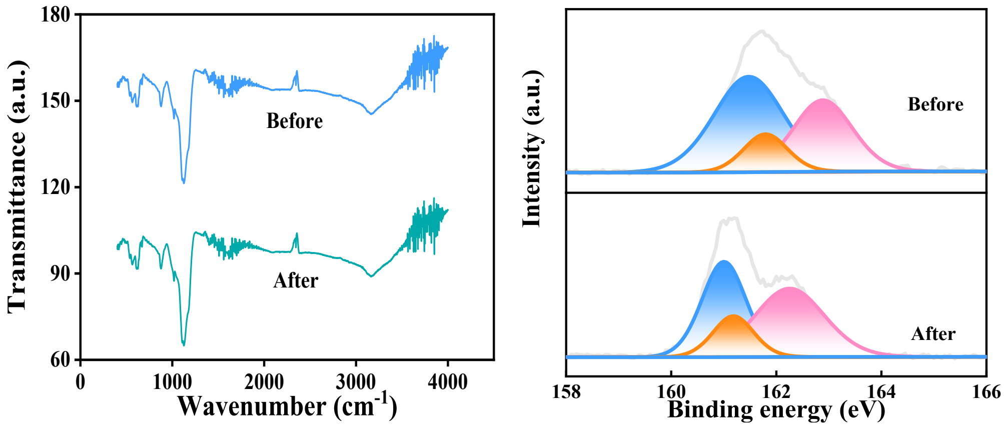

Figure S6. FT-IR and X-ray photoelectron spectroscopy of the catalyst after cycling.

References

[1] Shen, R., Ding, Y., Li, S., Zhang, P., Xiang, Q., Ng, Y. H., Li, X. (2021). Constructing low-cost Ni_3C/twin-crystal $Zn_{0.5}Cd_{0.5}S$ heterojunction/homojunction nanohybrids for efficient photocatalytic H_2 evolution. Chin. J. Catal., 42(1), 25-36.

[2] Zhang, X., Yuan, H., Bao, J., Xiao, W., He, G. (2023). Interfacial construction of SnS_2/$Zn_{0.2}Cd_{0.8}S$ nanopolyhedron heterojunctions for enhanced photocatalytic hydrogen evolution. J. Colloid Interface Sci., 651, 254-263.

[3] Zhao, S., Xu, J., Mao, M., Li, L., Li, X. (2020). $NiCo_2S_4$@ $Zn_{0.5}Cd_{0.5}S$ with direct Z-scheme heterojunction constructed by band structure adjustment of $Zn_xCd_{1-x}S$ for efficient photocatalytic H_2 evolution. Appl. Surf. Sci., 528, 147016.

[4] Zhang, Y., Lu, D., Li, H., Kondamareddy, K. K., Wang, H., Zhang, B., Wang, J., Wu, Q., Zeng, Y., Zhang, X., Zhou, M., D, N., Hao, H., Pei, H., Fan, H. (2022). Enhanced visible Light-Driven photocatalytic hydrogen evolution and stability for noble Metal-Free $MoS_2/Zn_{0.5}Cd_{0.5}S$ heterostructures with W/Z phase junctions. Appl. Surf. Sci., 586, 152770.

[5] Lou, Y., Fei, T., Zhang, Y., Dong, G., Deng, Q., Zhou, Y., Mao, C. (2022). Construction of 1D/0D/2D $Zn_{0.5}Cd_{0.5}S$/PdAg/g-C_3N_4 ternary heterojunction composites for efficient photocatalytic hydrogen evolution. Int. J. Hydrogen Energy, 47(5), 2936-2946.

[6] Ge, G., Yuan, S., Liu, Q., Yang, D., Shi, J., Lan, X., Xiao, K. (2022). Insight into the function of noble-metal free Cu_3P decorated $Zn_{0.5}Cd_{0.5}S$ for enhanced photocatalytic hydrogen evolution under visible light irradiation--mechanism for continuous increasing activity. Appl. Surf. Sci., 597, 153660.

[7] Du, X., Hu, J., Sun, Q., Fu, H., Zhang, J., Chang, J., Liao, Y. (2024). Rapid microwave preparation of CuS/ZnCdS Z-scheme heterojunction for efficient photocatalytic hydrogen evolution. Int. J. Hydrogen Energy, 51, 936-945.

[8] Fan, W., Chang, H., Zhong, J., Lu, J., Ma, G., Zhang, H., Yin, G. (2024). Facile synthesis of ZnCdS quantum dots via a novel photoetching MOF strategy for boosting photocatalytic hydrogen evolution. Sep. Purif. Technol., 330, 125258.

[9] Ma, S., Wang, X., Wan, K., Liu, B., Yang, Y., Wang, S. (2025). Metal-organic framework-derived $Zn_xCd_{1-x}S/Zn_xCd_{1-x}$-MOF heterostructures promoting charge separation for photocatalytic hydrogen evolution. Sep. Purif. Technol., 354, 129089.

[10] Zhang, R., Gong, K., Cao, S., Du, F. (2022). Amorphous sulfur-rich CoS_x nanodots as highly efficient cocatalyst to promote photocatalytic hydrogen evolution over TiO_2. Int. J. Hydrogen Energy, 47(94), 39875-39885.

[11] Ren, X., Shi, J., Duan, R., Di, J., Xue, C., Luo, X., Liu, Q., Xia M., Lin B., Tang, W. (2022). Construction of high-efficiency CoS@ Nb_2O_5 heterojunctions accelerating charge transfer for boosting photocatalytic hydrogen evolution. Chinese Chem. Lett., 33(10), 4700-4704.

[12] Feng, X., Shang, H., Zhou, J., Ma, X., Gao, X., Wang, D., Zhang, B., Zhao, Y. (2023). Heterostructured core–shell $CoS_{1.097}$@ $ZnIn_2S_4$ nanosheets for enhanced photocatalytic hydrogen evolution under visible light. Chem. Eng. J., 457, 141192.